Pergamon

0042-6989(94)00320-3

Vision Res. Vol. 35, No. 16, pp. 2245–2254, 1995

0042-6989/95 $9.50 + 0.00

A Four-surface Schematic Eye of Macaque Monkey Obtained by an Optical Method

PABLO LAPUERTA,*† STANLEY J. SCHEIN*‡§

Received 9 May 1994; in revised form 3 November 1994; in final form 12 December 1994

Schematic eyes for four *Macaca fascicularis* monkeys were constructed from measurements of the positions and curvatures of the anterior and posterior surfaces of the cornea and lens. All of these measurements were obtained from Scheimpflug photography through the use of a ray-tracing analysis. Some of these measurements were also checked (and confirmed) by keratometry and ultrasound. Gaussian lens equations were applied to the measured dimensions of each individual eye in order to construct schematic eyes. The mean total power predicted by the schematic eyes agreed closely with independent measurements based on retinoscopy and ultrasound results, 74.2 ± 1.3 (SEM) vs 74.7 ± 0.3 (SEM) diopters. The predicted magnification of 202 μm/deg in one eye was confirmed by direct measurement of 205 μm/deg for a foveal laser lesion. The mean foveal retinal magnification calculated for our eight schematic eyes was 211 ± (SEM) μm/deg, slightly less than the value obtained by application of the method of Rolls and Cowey [*Experimental Brain Research, 10,* 298–310 (1970)] to our eight eyes but just 4% more than the value obtained by application of the method of Perry and Cowey [*Vision Research, 12,* 1795–1810 (1985)].

Physiological optics Schematic Magnification Eye Macaque

INTRODUCTION

The purpose of this study was to construct a four-surface schematic eye for the macaque monkey. We described the eye as a series of four spherical surfaces separated by media of different indices of refraction, and we applied Gaussian lens equations to obtain the position of the posterior nodal point of the optical system (Southall, 1943). With our estimate of the position of the posterior nodal point and information on axial length we derived foveal retinal magnification.

We applied several techniques to obtain the positions and curvatures of the surfaces of the cornea and lens. In order to obtain some of the values for ocular dimensions we relied on standard procedures such as keratometry and ultrasound. However, to determine values of lens curvatures and posterior corneal curvature we used Scheimpflug photography and developed a means of analyzing our Scheimpflug photographs of the eye.

Scheimpflug photography (Scheimpflug, 1906) provides an image of a sagittal section of the eye (Fig. 1). The analysis of these photographs is complicated by the optics of the camera and by the existence of several different refracting surfaces in the eye. For example, in a photograph of the eye the apparent shape and size of the lens is affected not only by the optics of the camera, but also by the cornea, which magnifies the image of the lens.

Ray-tracing techniques have previously been used to analyze Scheimpflug photographs and account for the effects of refracting surfaces (Richards, Russell & Anderson, 1988; Kampfer, Wegener, Dragomirescu & Hockwin, 1989). Richards *et al.* (1988) used ray-tracing to study anterior chamber geometry. However, their study did not address characteristics of the posterior lens surface and provided no comparison to other techniques (such as ultrasound) in order to assess the accuracy of their analysis. Kampfer *et al.* (1989) also used a ray-tracing technique to analyze Scheimpflug photographs of a model eye. They analyzed how changes in the dimensions of the model eye affected their Scheimpflug data. They did not report their technique's accuracy in providing measurements of lens curvatures.

In this study we developed a ray-tracing technique along the lines of Richards *et al.* (1988) and Kampfer *et al.* (1989). To establish the accuracy of our Scheimpflug technique we compared its results to those obtained from keratometry and ultrasound. We further assessed the validity of our technique by testing the accuracy of the schematic eye's predictions of total power and retinal magnification.

We also compared our estimates of magnification to those obtained by the methods of Rolls and Cowey (1970) and Perry and Cowey (1985) on our monkeys.

*Department of Psychology, University of California, Los Angeles, Los Angeles, CA 90095-1563, U.S.A.
†Present address: University of Southern California School of Medicine, Department of Internal Medicine, AHC 133, 1355 San Pablo Street, Los Angeles, CA 90033, U.S.A.
‡Brain Research Institute, University of California, Los Angeles, Los Angeles, CA 90095, U.S.A.
§To whom all correspondence should be addressed.

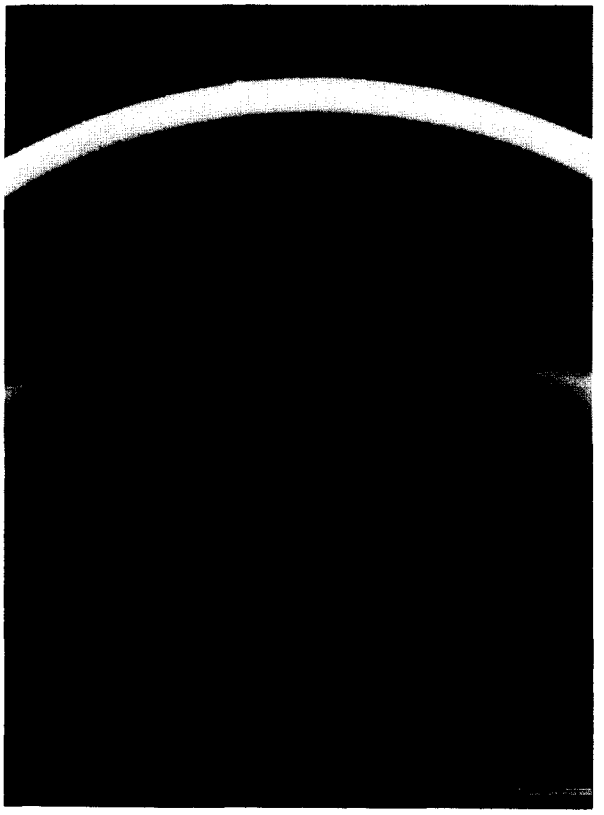

FIGURE 1. Scheimpflug photograph of the eye. A sagittal section of the eye is seen and the entire sagittal plane is in focus. Calibration bar = 1 mm. This calibration may be applied directly to the anterior surface of the cornea. However, the sizes of the images of the posterior cornea and the lens have been affected by the surfaces which lie between them and the camera.

Rolls and Cowey (1970) obtained a magnification estimate of 246 μm/deg for *Macaca mulatta*, and Perry and Cowey (1985) obtained estimates of 223 μm/deg for *Macaca mulatta* and 200.7 μm/deg for *Macaca fascicularis*. Lacking measurements of lens curvatures, these investigators were forced to guess the location of the posterior nodal point, which they did by assuming similarities between the macaque and human eyes. Our approach differed from the previous work of Rolls and Cowey (1970) and Perry and Cowey (1985) because a more complete set of optical measurements enabled us to identify posterior nodal points by constructing schematic eyes.

MATERIALS AND METHODS

Ocular measurements

We studied eight eyes of 4 female cynomolgus monkeys (*Macaca fascicularis*), one 5-yr-old male and three 11 to 12-yr-old females. The weights ranged from 3 to 4.5 kg. All animal procedures were performed in accordance with protocol approved by the university's animal care and use committee. For the performance of keratometry and ultrasound the monkeys were anesthetized with Ketamine (10 mg/kg) and Xylazine (1 mg/kg). Xylazine was supplemented (0.5 mg/kg) as needed. Drops of 0.5% cyclopentolate ophthalmic solution were used to dilate the pupils and produce an unaccommodated state. Drops of 1% proparacaine were used to provide topical anesthesia to the cornea. Measurements of anterior corneal curvature were made with a Bausch & Lomb keratometer (model No. 71-21-35). Measurements of anterior chamber depth, lens thickness, and axial length were made with the Acron Surgical Digital B-4000 ultrasound machine. Measurements of corneal thickness were made with the Alkon Surgical Biophysics Mini-A ultrasound machine. Several photographs were made of each eye with the Topcon SL-45 Scheimpflug camera.

In order to obtain refractive error, retinoscopy was also performed on the four monkeys. Drops of atropine ophthalmic solution were used to dilate the pupils and produce an unaccommodated state. The subjects were sedated with Ketamine (10 mg/kg), which was supplemented (5 mg/kg) as needed. Streak retinoscopy was performed with a Welch Allyn retinoscope to identify the reversal point or the best corrective lens for each eye.

In one of the subjects measurements of retinal magnification were made on the basis of a retinal laser lesion established in a previous procedure. In this procedure the macaque monkey was sedated with Ketamine (10 mg/kg) and surgically anesthetized with sodium pentobarbital (20 mg/kg). Sodium pentobarbital was supplemented (5 mg/kg) as needed, based on changes in heart rate, blood pressure, and the response to pinch. Heart rate and blood pressure were measured every 3 min. Paralysis was obtained with Flaxedil, and respiration was maintained with a mixture of 50% N_2O and 50% O_2. The respiratory rate was adjusted to maintain a fraction of expired CO_2 of approximately 4.5%.

The red (647 nm) light of a krypton laser was used to make the lesion. The laser was connected to a rod extending from the subject's stereotaxic holder and pivoted about the approximate location of the anterior nodal point of the eye. The laser lesion spanned a distance of 12 deg of visual field and was centered around the fovea.

At a later date, after retinoscopy, ultrasound, keratometry, and Scheimpflug photography had been performed, the subject was sacrificed by an overdose of sodium pentobarbital (100 mg/kg) and perfused with a soft fixative, phosphate buffered (pH 7.4), isotonic 3% paraformaldehyde. The retina was removed and reacted in whole mount for a mitochondrial enzyme, cytochrome oxidase. This method of fixation and removal of the retina has been previously evaluated for shrinkage, which was found to be negligible (De Monasterio, McCrane, Newlander & Schein, 1985; Schein, 1988).

The span of the laser lesion was measured. The length of the span on the retina (in μm) was divided by the corresponding value of 12° of visual field to obtain a measurement of magnification (μm/deg). This approach to measuring magnification was similar to that of Frisén and Schöldström (1976), who measured both the visual field span and retinal distance between laser lesions in a human eye.

Analysis of Scheimpflug photographs

When Scheimpflug photography was performed several photographs were taken of each eye. We chose three 35 mm negatives for each eye, selecting them on the basis of the visibility of the posterior lens. We made 8 × 10″ calibrated enlargements from these negatives and based our analysis on measurements from these photographs. In order to obtain single estimates of ocular dimensions for each eye we averaged the results of each group of three photographs.

We approached our analysis by considering the 35 mm negative to represent the "image plane" of the camera. The actual position of the illuminated sagittal section of the eye in three-dimensional space provided the "object plane." This relationship between the image plane and the object plane was previously described by Richards *et al.* (1988) and is illustrated in Fig. 2. In order to obtain values for lens curvatures and other ocular dimensions our goal was to find the object plane origins of rays of light which created the image of the macaque eye in the image plane.

Coordinates for seven points each on the anterior corneal, posterior corneal, anterior and posterior lens surfaces were obtained by placing a grid over the 8″ × 10″ prints made from the 35 mm negatives and correcting for the enlargement factor. Our sets of seven points covered a span corresponding to 3–4 mm on the negative, which in turn was equivalent to a span of 3–4 mm on the anterior corneal surface (magnification of the anterior corneal surface was approx 1 ×).

We used these sets of image plane points in a computer program which traced rays of light from the image plane to the object plane. Each ray was initially defined by two points, its image plane point and the nodal point of the camera. By following rays through the nodal point to the object plane we corrected for camera distortion.

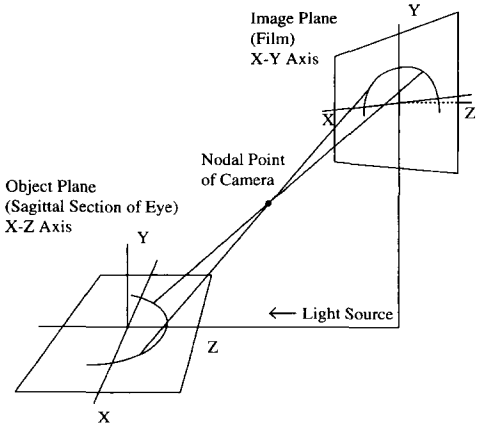

FIGURE 2. Coordinate system for the analysis of Scheimpflug photographs. With the Scheimpflug technique the image plane and the object plane are perpendicular to each other. The light source is placed in front of the eye, whereas the camera is located to the side at an angle of 45°. This arrangement allows a side view of a sagittal section of the eye (figure after Richards *et al.*, 1988). The nodal point of the camera is 88.92 mm from the origin of the image plane.

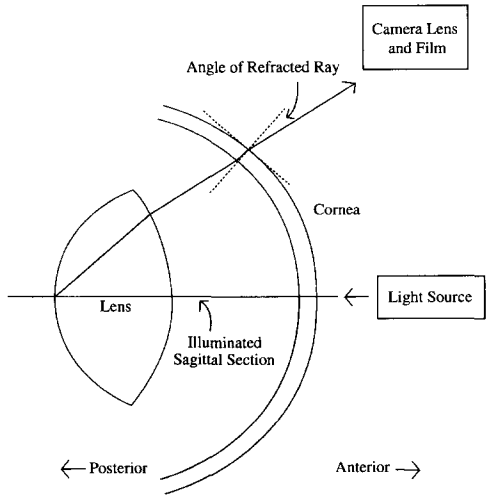

FIGURE 3. Ray from the posterior lens surface, refracted several times before reaching the Scheimpflug camera. Light from the illuminated sagittal section of the posterior lens surface is refracted by the anterior lens, posterior corneal, and anterior corneal surfaces before reaching the camera. In order to trace the ray from the posterior lens Snell's law is applied at each refracting surface. A similar approach is required to trace rays from the anterior lens and posterior corneal surface.

With the anterior cornea this correction for camera distortion was the only correction needed. The points of origin of these rays in the object plane were determined, and a circle was fitted to these seven points of origin by a least squares fit. Surface "curvature" was the radius of curvature of the circle fitted to the surface's object plane points.

In order to measure the curvature and position of the posterior corneal surface we considered the refraction of its image caused by the anterior corneal surface. The general strategy we used is described in Figs 3 and 4. Rays were followed from the seven points in the image plane through the camera's nodal point to the anterior corneal surface. At the points of intersection with the anterior cornea the angles of incidence and refraction were determined by Snell's law, allowing a calculation of the directions of the original rays from the posterior cornea. With a set of seven points representing the posterior cornea in the object plane we applied the least squares fit to find the curvature and position of the posterior surface of the cornea.

The same strategy was applied to the anterior and posterior lens surfaces. Each point from the image plane was traced through the camera's nodal point and through the intermediate refracting surfaces, with Snell's law applied at each surface to account for the change in direction of the ray (Figs 3 and 4).

In applying Snell's law we assumed an index of refraction of 1.3771 for cornea and 1.42 for lens (Le Grand & El Hage, 1980). For the aqueous and vitreous humor in the monkey we used a refractometer and obtained refractive indices of 1.336 for both, the same values presented in Gullstrand's No. 1 schematic eye (Southall, 1943).

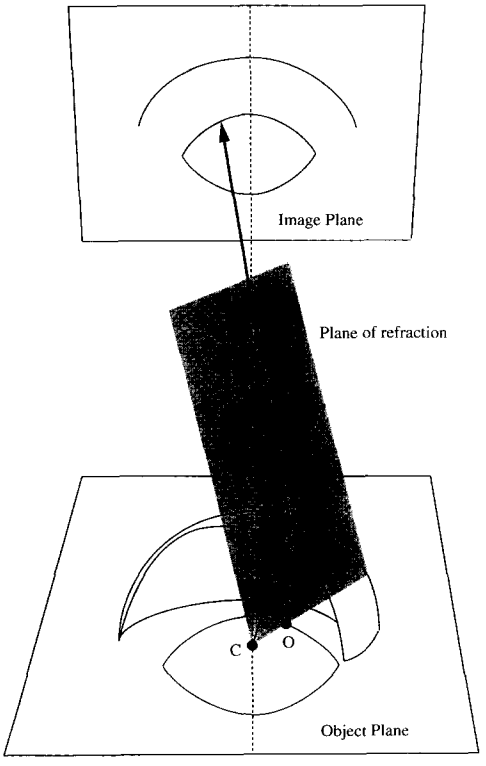

FIGURE 4. Use of a 3-dimensional coordinate system in ray-tracing. In Scheimpflug photography the object plane, which is a mid-sagittal section of the eye, is at right angles to the image plane, which is the plane of the negative. In this illustration an incoming ray of light (not shown) has been reflected by the anterior lens surface (in the object plane). The outgoing ray from the anterior lens surface is refracted by the anterior corneal surface before reaching the negative. (The posterior corneal surface is omitted to allow a simple description of the system.) Ray-tracing is accomplished by following this reflected ray backwards from the image point of the negative through the nodal point N of the camera and through the refracting surfaces of the eye until the location of its origin O in the object plane is determined. Point C is the center of curvature of the cornea, which lies in the object plane (the mid-sagittal section of the eye). S is the intersection of the ray and the cornea. Together, points C, S, and N define the plane of refraction (shaded surface). The angle of refraction r is equal to 180° minus $\angle$CSN. The angle of incidence is derived from Snell's law. Ray-tracing is performed within the plane of refraction.

Construction of schematic eyes

In order to construct schematic eyes we assembled complete sets of the positions and curvatures of the refractive surfaces of the eye. We applied Gaussian lens equations to these results in order to estimate total power, focal lengths, and the positions of the principal points and nodal points.

In applying Gaussian lens equations we used a strategy outlined by Southall (1943). The principle was to describe the refracting surfaces of the eye as one combined optical system, which has a total power, anterior and posterior focal points, principal points (analogous to the position of a lens), and nodal points (analogous to the center of curvature of a lens). The description of this combined optical system, along with the ocular dimensions of its components, constituted the schematic eye. Southall's (1943) textbook provided the necessary lens equations and described in detail the steps required for assembly of a schematic eye.

With this approach we developed three types of schematic eyes based on different sets of ocular dimensions. We called the first type the "combined" schematic eye. It was based on the results of different techniques. Keratometry provided anterior corneal curvature. Ultrasound provided corneal thickness, anterior chamber depth, and lens thickness. Scheimpflug photography provided posterior corneal curvature and anterior and posterior lens curvatures. There were eight "combined" schematic eyes, one for each individual eye studied.

We called the second type of schematic eye the "representative" schematic eye. There was only one "representative" eye constructed, and it was based on the average ocular dimensions which we used in construction of the "combined" schematic eyes. The "representative" eye was based on average ocular dimensions in order to illustrate typical features of the eight *Macaca fascicularis* eyes we studied.

We also wished to determine whether Scheimpflug photography alone could provide a valid schematic eye, so we developed a third type of schematic eye, the "all Scheimpflug" eye. Whereas the "combined eye" depended on results of several techniques, the "all Scheimpflug" eye was based solely on the results of Scheimpflug photography. We assembled eight "all Scheimpflug" schematic eyes, one for each subject eye studied.

Estimates of retinal magnification

Each schematic eye was associated with an estimate of foveal magnification. Although the fovea is slightly off the optic axis (Bennett & Rabbetts, 1984), we estimated foveal magnification by calculating magnification at the posterior pole. At the posterior pole radial and circumferential magnifications (Drasdo & Fowler, 1974) were identical, so each estimate of foveal magnification was presented as a single result (in units of μm/deg). We use the general term "magnification" to refer to foveal magnification, unless otherwise stated.

Calculations of magnification were made according to the equations of Drasdo and Fowler (1974). The necessary elements for calculating magnification were the axial length of the eye and the position of the posterior nodal point. We assumed that the radius of the retina is one half of axial length.

Tests of the schematic eyes

We first evaluated our schematic eyes by examining the accuracy of individual Scheimpflug measurements. We had obtained values of anterior corneal curvature by both Scheimpflug photography and keratometry, so we compared the results of these two techniques. For each of the eight eyes we paired our Scheimpflug measurement of anterior corneal curvature with the corresponding keratometry measurement and obtained the difference between the two. Our null hypothesis was that the mean difference between the paired measurements was zero. The paired t-test was used to obtain a P-value indicating the probability that the null hypothesis was correct.

The same approach was applied to compare Scheimpflug and ultrasound measurements. Both procedures had provided data on corneal thickness, anterior chamber depth, and lens thickness. For each of these dimensions we paired the Scheimpflug and ultrasound results, and we used the t-test to evaluate the null hypothesis that the mean difference between Scheimpflug photography and ultrasound was zero.

A second means of evaluating the schematic eyes was to compare our predictions of total power to independent calculations based on an approach provided by Bennett and Rabbetts (1984). We used their equations, applying axial length measurements (made from ultrasound) and measurements of refractive error (determined from retinoscopy) to make independent calculations of total power. We compared these results to the predictions of the schematic eyes.

A third test involved the analysis of a retinal laser lesion [Fig. 5(A)] in one eye of the subject which was sacrificed. Measurement of the retinal laser lesion in that eye after sacrifice [Fig. 5(B)] provided an independent, direct measurement of foveal retinal magnification. This

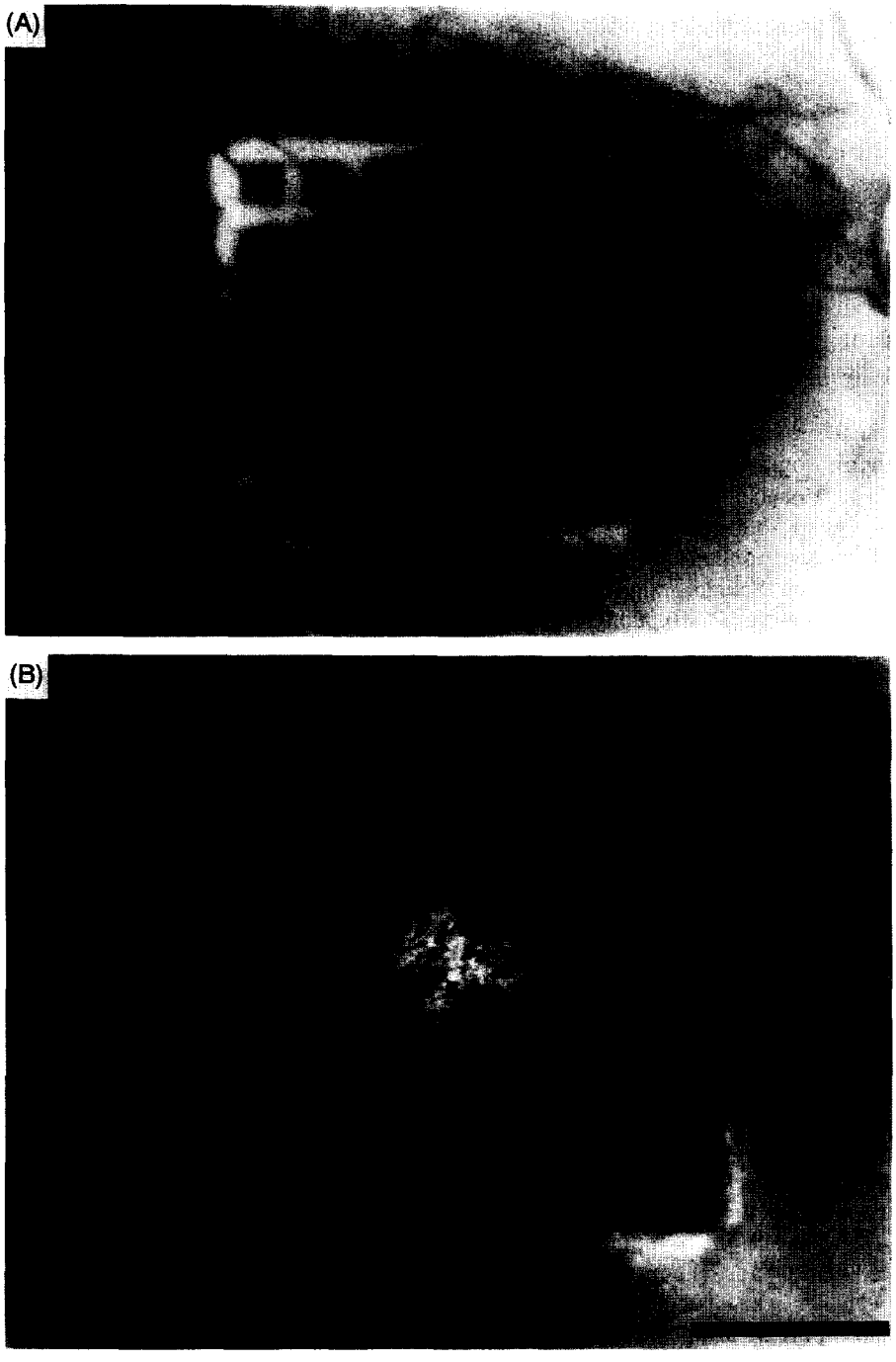

FIGURE 5. Fundus photograph of the left eye of macaque No. 7-81 immediately after creation of a retinal laser lesion (A) and after sacrifice and histochemical reaction for the cytochrome oxidase enzyme (B). The outermost lines are located at a position of 6 deg from the fovea. Calibration bar = 1 mm.

measurement was compared to the predictions of magnification derived from that eye's "combined" and "all Scheimpflug" schematic eyes.

The method of Rolls and Cowey (1970) for estimating magnification was applied to the eight eyes studied by assuming that the ratio of the distance between the posterior nodal point and posterior pole to axial length was the same as in Gullstrand's No. 1 human schematic eye, 0.69 (Southall, 1943). The method of Perry and Cowey (1985) was applied by assuming that the posterior nodal point was approx. 0.1 mm behind the posterior lens surface, whose position was identified from ultrasound results. The equations of Drasdo and Fowler (1974) were applied to these estimates of posterior nodal point position in order to estimate magnification.

RESULTS

Values for anterior corneal curvature, corneal thickness, anterior chamber depth and lens thickness obtained from Scheimpflug photography are compared to the results of keratometry and ultrasound in Fig. 6(A–D). In Table 1 the mean differences between the Scheimpflug results and the alternate techniques are presented, along with P-values indicating the probability that the difference between the Scheimpflug results and the alternate technique is zero.

For anterior corneal curvature the mean difference between Scheimpflug photography and keratometry was only 0.04 mm (Table 1). For axial dimensions of the eye Scheimpflug results tended to be slightly greater than ultrasound results. For measurements of corneal thickness the difference between Scheimpflug photography and ultrasound was significant ($P = 0.0005$).

The Scheimpflug photograph results included a mean radius of curvature of 5.12 mm for the posterior corneal surface. For the anterior and posterior lens surfaces the mean curvatures were 10.34 and 6.39 mm, respectively.

The average total power of the eight "combined" schematic eyes assembled from ultrasound, keratometry, and Scheimpflug data was 75.2 ± 1.5 (SEM) D. Based on the axial lengths and locations of the posterior nodal point, the average predicted magnification for these eight eyes was 213 ± 3 (SEM) μm/deg. The one "representative" schematic eye, based on the average ocular dimensions of the "combined" eyes, is presented in Fig. 7. Its total power is 74.2 D and its magnification is 212 μm/deg.

The eight "all-Scheimpflug" schematic eyes based solely on the results of Scheimpflug photography had an average total power of 74.2 ± 1.3 (SEM) D. The average predicted magnification from these schematic eyes was 211 ± 3 (SEM) μm/deg. Predictions of magnification for individual "combined" and "all-Scheimpflug" eyes are presented in Table 2.

Independent calculations of total power based on retinoscopy and ultrasound results yielded an average value of 74.7 ± 0.3 (SEM) D. These individual measurements are compared to the predicted total powers of the individual "combined" and "all-Scheimpflug" schematic eyes in Fig. 8.

In the eye whose laser lesion was evaluated, 781L, we found a radial retinal magnification of 205 μm/deg over the 12° span of the lesion (which was centered on the fovea). For that subject the individual "combined"

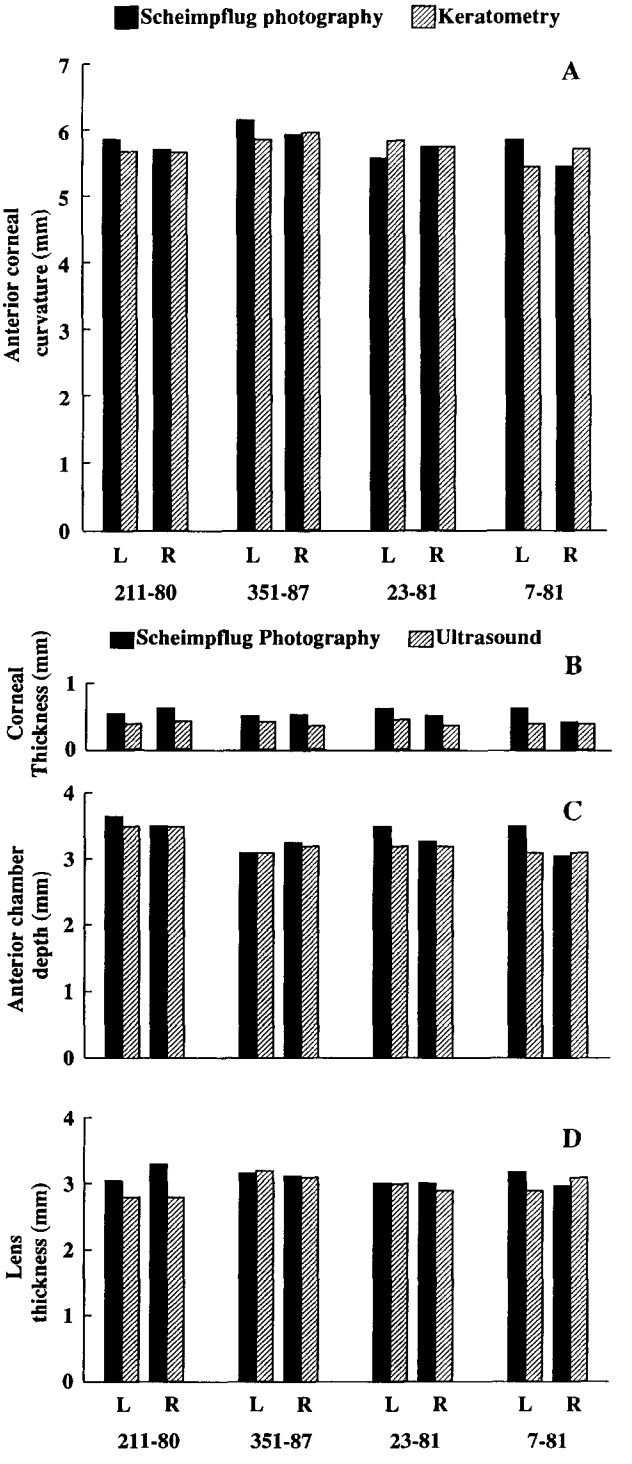

FIGURE 6. Scheimpflug results compared to results of keratometry and ultrasound. (A) Scheimpflug compared with keratometry values of anterior corneal curvature. (B–D) Scheimpflug and ultrasound results for corneal thickness, anterior chamber depth, and lens thickness, respectively. The labels for the eyes include a number representing the monkey and a letter indicating the side where the eye is located. For example, 21180L and 21180R are the left and right eyes of monkey No. 211-80.

TABLE 1. Scheimpflug values for ocular dimensions compared to the results of keratometry and ultrasound. The paired t-test was used to provide the P-value indicating the probability that the difference between Scheimpflug measurements and those of the alternate technique was zero

	Average Scheimpflug result (mm)	Average result of alternate technique (mm)	Difference (mm)	P-Value
Anterior corneal curvature	5.80	5.75 (keratometry)	0.04	0.6
Corneal thickness	0.55	0.40 (ultrasound)	0.15	0.0005
Anterior chamber depth	3.35	3.24 (ultrasound)	0.12	0.08
Lens thickness	3.10	2.98 (ultrasound)	0.12	0.1

schematic eye predicted a foveal magnification of 210 μm/deg, and the "all-Scheimpflug" schematic eye predicted a foveal magnification of 202 μm/deg.

The method of Rolls and Cowey (1970), when applied to the eight *Macaca fascicularis* eyes that we studied, produced an average magnification estimate of 217 ± 4 (SEM) μm/deg. The method of Perry and Cowey (1985) produced an average magnification of 203 ± 2 (SEM) μm/deg.

DISCUSSION

Validation of the Scheimpflug method

The ocular dimensions obtained from Scheimpflug photography were in excellent agreement with the corresponding dimensions obtained from keratometry and ultrasound. Predictions of total power from the schematic eyes agreed with independent measurements based on retinoscopy and ultrasound (Fig. 8). The direct

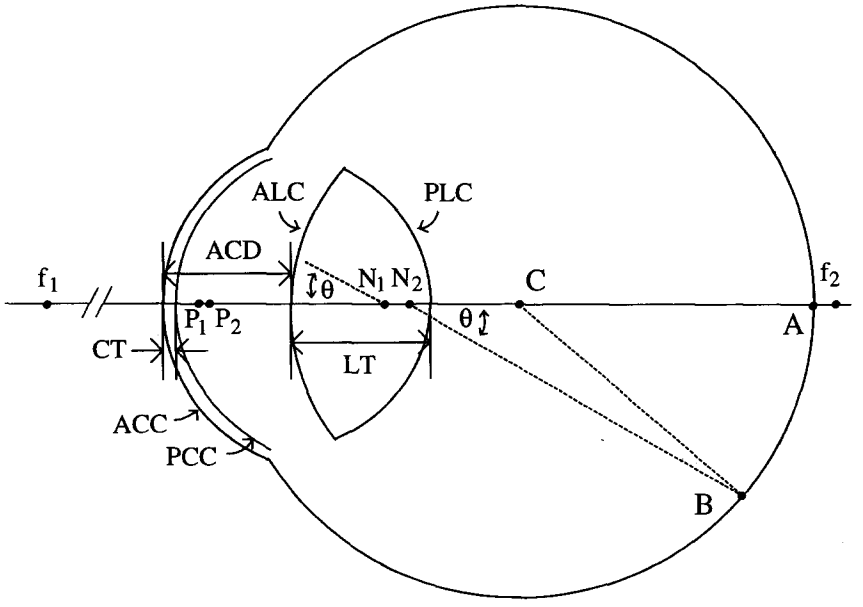

AVERAGE OCULAR DIMENSIONS			OPTICAL PARAMETERS		
Anterior Corneal Curvature	ACC	5.75	Anterior Principal Point	P_1	-1.03
Posterior Corneal Curvature	PCC	5.12	Posterior Principal Point	P_2	-1.22
Corneal Thickness	CT	0.4	Anterior Nodal Point	N_1	-5.56
Anterior Chamber Depth	ACD	3.24	Posterior Nodal Point	N_2	-5.75
Anterior Lens Curvature	ALC	10.34	Posterior Nodal Distance	PND	12.17
Posterior Lens Curvature	PLC	6.39	Anterior Focal Length	$\overline{f_1P_1}$	13.48
Lens Thickness	LT	2.98	Posterior Focal Length	$\overline{f_2P_2}$	18.01
Axial Length		17.92	Total Power		74.2 D
			Retinal Magnification		212 μm/deg

FIGURE 7. The "representative" schematic eye. This schematic eye is derived by applying Gaussian lens equations to mean ocular dimensions of the "combined" eyes. For construction of the schematic eye we used indices of refraction of 1.3771 for cornea, 1.336 for aqueous and vitreous humor, and 1.42 for the lens. Point locations are presented with respect to the position of the anterior vertex of the cornea. The estimate of magnification comes from the equations of Drasdo and Fowler (1974), who considered a ray of light (with visual field position θ) passing through the posterior nodal point N_2 at the angle θ with the optic axis. Arclength $\widehat{AB}$ is the distance of the retinal image from the posterior pole:

$$\widehat{AB} = \frac{\pi R}{180}\left[\theta + \arcsin\left(\frac{\overline{N_2C}\sin(\theta)}{R}\right)\right].$$

Although the fovea is slightly off the optic axis, we estimate magnification by calculating $d\widehat{AB}a/d\theta$ at the posterior pole ($\theta = 0$):

$$\text{foveal mag.} = \frac{\pi}{180}[R + \overline{N_2C}].$$

TABLE 2. Foveal retinal magnification for the "combined" and "all-Scheimpflug" schematic eyes. Magnification is derived from posterior nodal point position and axial length (see legend of Fig. 7). Posterior nodal point position is given in reference to the anterior vertex of the cornea. The negative signs indicate that the posterior nodal points are located behind (posterior to) the anterior vertex of the cornea

		"Combined" schematic eyes		"All-Scheimpflug" schematic eyes	
Eye	Axial length (mm)	Posterior nodal point position (mm)	Foveal retinal magnification (μm/deg)	Posterior nodal point position (mm)	Foveal retinal magnification (μm/deg)
L21180	18.35	−5.70	221	−5.91	217
R21180	18.39	−5.54	224	−5.83	219
L35187	17.98	−5.87	211	−6.09	208
R35187	17.68	−5.92	205	−5.90	206
L2381	18.08	−5.83	214	−5.66	217
R2381	18.11	−5.79	215	−5.81	215
L781	17.46	−5.43	210	−5.91	202
R781	17.29	−5.76	201	−5.48	206
Average	17.92	−5.73	213	−5.82	211

measurement of a retinal laser lesion in one of the eyes provided a value of retinal magnification which was similar to the prediction of its individual schematic eye. These results suggest that our ray-tracing analysis of Scheimpflug photographs was accurate and that the schematic eyes were valid.

The "all-Scheimpflug" eyes and the "combined" eyes provided similar results. The average total power for the two sets of schematic eyes was only 1 D apart, and the average result from ultrasound and retinoscopy was between the two. Average retinal magnifications for the two sets of schematic eyes were almost identical (213 μm/deg for the "combined" eyes and 211 μm/deg for the "all-Scheimpflug" eyes). The similarity of the two sets suggests that Scheimpflug photography alone is sufficient for predicting total power, and when combined with axial length information it can predict retinal magnification.

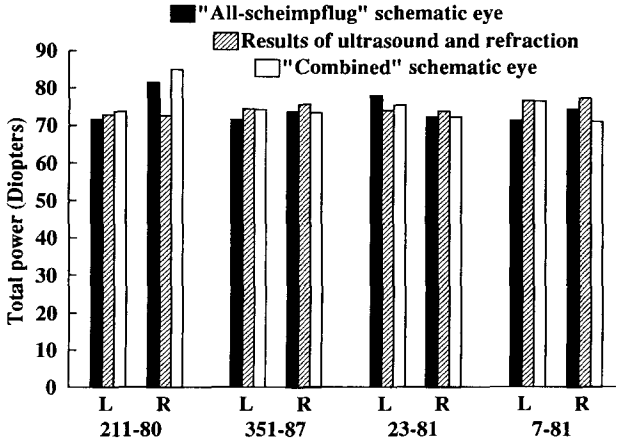

FIGURE 8. Comparison of total power from "all-Scheimpflug" schematic eyes, from calculations based on ultrasound and retinoscopy results, and from "combined" schematic eyes. The "combined" schematic eye is based on results of keratometry (anterior corneal curvature), ultrasound (corneal thickness, anterior chamber depth, and lens thickness), and Scheimpflug photography (anterior and posterior lens curvatures and posterior corneal curvature). The "all-Scheimpflug" schematic eye is based solely on the Scheimpflug technique.

One reason for the similarity between the "combined" and "all-Scheimpflug" schematic eyes is the accuracy of the Scheimpflug technique's measurements of anterior corneal curvature. Scheimpflug results for corneal thickness, anterior chamber depth, and lens thickness tended to be greater than ultrasound results, but these differences did not have a significant effect on the schematic eye because anterior corneal curvature is the most important determinant of the eye's total power. In any case, mean differences in Scheimpflug photography and ultrasound results were only on the order of 0.12–0.15 mm, which is small, considering that our ultrasound machines only provided measurements to within 0.1 mm.

Potential refinements of the schematic eye

A model which is more accurate than our four-surface schematic eye could be developed by increasing the sophistication of the description of the lens. In the human (Southall, 1943) and in the rat (Hughes, 1978) schematic eyes have been described which separate the lens into two parts, an inner cortex and an outer core. In other studies the lens has been described by a continuous refractive index gradient (Campbell and Hughes, 1981) or a series of many different layers (Pomerantzeff, Pankratov, Wang & Dufault, 1984). In this study we have considered the lens to consist of only two refracting surfaces separated by a uniform media with one index of refraction. Knowledge of the refractive index gradient in macaque could provide a more accurate description of the power of the lens and may also provide better estimates of posterior lens curvatures.

Describing the cornea as an ellipse (Drasdo & Fowler, 1974) might also allow a better description of the optics of the macaque eye, but such an approach would necessarily eliminate the use of Gaussian lens equations, which apply only to spherical surfaces. No clear focal point or nodal point would be defined.

The use of the Scheimpflug technique in studying visual optics

The Scheimpflug technique can serve as a helpful tool because it obtains important optical information *in vivo*, without the requirement of enucleation and post-mortem examination. Many studies on the schematic eye in other animals refer to post-mortem lens data (Hughes, 1972; Massof & Chang, 1972; Hughes, 1977; Remtulla & Hallett, 1985; Mathis, Schaeffel & Howland, 1988; Sivak, Howland, West & Weerheim, 1989; McBrien & Norton, 1992a, b; Troilo, Howland & Judge, 1993). Other optical studies use post-mortem examination of the retina to measure magnification or posterior nodal distance (Hughes, 1976; Freeman and Tancred, 1978; Kooijman, 1983; Schaeffel, Glasser & Howland, 1988). Application of the Scheimpflug technique may be useful in optical studies where post-mortem examination of either the retina or lens is not feasible, or where there is concern that enucleation, post-mortem changes, or processing may introduce significant distortion in the shape of the lens or retina.

Other methods of estimating retinal magnification in macaque

The development of schematic eyes can be used in order to obtain estimates of retinal magnification. However, the careful analysis required to analyze Scheimpflug photography requires a considerable amount of effort. Our findings can shed light on prior efforts to obtain magnification in macaque monkey and can suggest some additional, simple approaches to estimating retinal magnification.

The method of Rolls and Cowey (1970) provided estimates very close to those of our "combined" schematic eyes [217 ± 4 (SEM) vs 213 ± 3 (SEM) μm/deg]. For our "combined" schematic eyes the ratio of the distance between the posterior nodal point and the posterior pole to axial length was 0.68, which was almost the same as the 0.69 ratio in Gullstrand's No. 1 human schematic eye (Southall, 1943). Rolls and Cowey's own published estimate of 246 μm/deg for *Macaca mulatta* was substantially different from ours because they adopted an axial length of 20 mm for *Macaca mulatta* eyes. Our eight *Macaca fascicularis* eyes had an average axial length of 17.92 mm determined by ultrasound.

The method of Perry and Cowey (1985) applied to the eight eyes in our study also provided estimates similar to those of the schematic eyes. The mean estimate of 203 ± 2 (SEM) μm/deg obtained by their method was within 5% of our "combined" schematic eyes' 213 ± 3 (SEM) μm/deg. However, individual estimates were consistently lower by their method. The difference exists because Perry and Cowey (1985) assumed that in the macaque eye the posterior nodal point lies behind the posterior lens surface (as in the human). We found instead that the posterior nodal point was located 0.5 mm in front of the posterior lens surface (Fig. 7) in our schematic eyes of *Macaca fascicularis*.

The schematic eyes developed in our study provided direct calculations of posterior nodal point position, rather than estimates based on assumed similarities with the human eye. Nevertheless, the methods of Rolls and Cowey (1970) and Perry and Cowey (1985) are practical because they are much easier to apply. From our results we can also propose two other methods which may be useful for estimating magnification.

The results of our study suggest that measurements of anterior corneal curvature alone may provide reasonable estimates of magnification. The cornea is the most powerful refracting surface of the eye, so the nodal point (analogous to center of curvature) of the eye's optical system may lie close to the center of curvature of the cornea. For our eight *Macaca fascicularis* eyes the difference between the two points is very small (0.04 mm on average), and the use of anterior corneal curvature as the sole indicator of nodal point position provides individual estimates of magnification which are essentially identical to the results of the schematic eyes.

Another alternative is to apply measurements of axial length (obtained from ultrasound) and total power (from retinoscopy) to an expression for magnification which we derive from the work of Southall (1943) and Drasdo and Fowler (1974). The derivation begins with a Gaussian lens equation which describes the distance $\overline{N_2C}$ in terms of $\overline{P_2N_2}$ (Fig. 7):

$$\overline{N_2C} = R - \overline{P_2N_2} - 1200.$$

The number 1200 comes from our average estimate (in μm) of posterior principal point position in *Macaca fascicularis* (Fig. 7).

$\overline{P_2N_2}$ is then described as a function of total power (D):

$$\overline{P_2N_2} = \frac{1.336 \cdot 10^6}{\text{Total power}} - \frac{10^6}{\text{Total power}}.$$

The expression for $\overline{P_2N_2}$ is substituted into the equation for $\overline{N_2C}$, and R is estimated to be one half of axial length. The expression for $\overline{N_2C}$ is in turn substituted into the magnification equation from the legend of Fig. 7 to complete the derivation:

$$\text{Foveal mag.} = \frac{\pi}{180}\left[\text{Axial length} - \frac{1.336 \cdot 10^6}{\text{Total power}} + \frac{10^6}{\text{Total power}} - 1200\right].$$

In this manner magnification is calculated from ultrasound and retinoscopy results. For the eight eyes studied this method provides the same average magnification estimate as the schematic eyes. In humans it can be applied if the value 1200 is replaced by 1600 to reflect the posterior principal point position provided in Southall's (1943) description of the Gullstrand No. 1 eye.

Comparison to a previous schematic eye of monkey

Vakkur (1967) derived a schematic eye for the monkey, and the results are presented in a table found in the *Handbook of Sensory Physiology* (Hughes, 1977).

The species of monkey studied is not given. An axial length of 17.97 mm is provided, which is similar to our average of 17.92 mm.

From the axial length and total power (82.916 D) provided, the equations of Bennett and Rabbetts (1984) suggest that Vakkur's monkey was nearsighted by 8.97 D in the unaccommodated state. In contrast, retinoscopy results showed that our unaccommodated monkeys were not significantly myopic.

Vakkur's (1967) estimate of magnification (250 μm/deg) also differs from the value we directly measured from a laser lesion (205 μm/deg). The parameters of Vakkur's eye do not agree with our independent measurements, even though they pertained to an eye of similar axial length.

REFERENCES

Bennett, A. G. & Rabbetts, R. B. (1984). *Clinical visual optics*. London: Butterworths.

Campbell, M. C. W. & Hughes, A. (1981). An analytic, gradient index schematic lens and eye for the rat which predicts aberrations for finite pupils. *Vision Research, 21*, 1129–1148.

De Monasterio, F. M., McCrane, E. P., Newlander, J. K. & Schein, S. J. (1985). Density profile of blue-sensitive cones along the horizontal meridian of macaque retina. *Investigative Ophthalmology and Visual Science, 26*, 289–302.

Drasdo, N. & Fowler, W. (1974). Non-linear projection of the retinal image in a wide-angle schematic eye. *British Journal of Ophthalmology, 58*, 709–713.

Freeman, B. & Tancred, E. (1978). The number and distribution of ganglion cells in the retina of the brush-tailed possum. *Journal of Comparative Neurology, 177*, 557–568.

Frisén, L. & Schöldström, G. (1977). Relationship between perimetric eccentricity and retinal locus in a human eye: Comparison with theoretical calculations. *Acta Ophthalmologica, 55*, 63–68.

Hughes, A. (1972). A schematic eye for the rabbit. *Vision Research, 12*, 123–138.

Hughes, A. (1976). A supplement to the cat schematic eye. *Vision Research, 16*, 149–154.

Hughes, A. (1977). The topography of vision in mammals. In Autrum, H., Jung, R., Loewenstein, W. R., MacKay, D. M. & Teuber, H. L. (Eds), *Handbook of Sensory Physiology 7(5)*, Berlin: Springer.

Hughes, A. (1978). A schematic eye for the rat. *Vision Research, 19*, 569–588.

Kampfer, T., Wegener, A., Dragomirescu, V. & Hockwin, O. (1989). Improved biometry of the anterior eye segment. *Ophthalmic Research, 21*, 239–248.

Kooijman, A. C. (1983). Light distribution on the retina of a wide-angle theoretical eye. *Journal of the Optical Society of America, 73*, 1544–1550.

Le Grand, Y. & El Hage, S. G. (1980). *Physiological optics*. Berlin: Springer.

McBrien, N. A. & Norton, T. T. (1992a). Normal development of refractive state and ocular component dimensions in the tree shrew (*Tupaia belangeri*). *Vision Research, 32*, 833–842.

McBrien, N. A. & Norton, T. T. (1992b). The development of experimental myopia and ocular component dimensions in monocularly lid-sutured tree shrews (*Tupaia belangeri*). *Vision Research, 32*, 843–852.

Massof, R. W. & Chang, F. W. (1972). A revision of the rat schematic eye. *Vision Research, 12*, 793–796.

Mathis, U., Schaeffel, F. & Howland, H. C. (1988). Visual optics in toads (*Bufo americanus*). *Journal of Comparative Physiology A, 163*, 201–213.

Perry, V. H. & Cowey, A. (1985). The ganglion cell and cone distributions in the monkey's retina: Implications for central magnification factors. *Vision Research, 12*, 1795–1810.

Pomerantzeff, O., Pankratov, M., Wang, G. & Dufault, P. (1984). Wide-angle optical model of the eye. *American Journal of Optometry and Physiological Optics, 61*, 166–176.

Remtulla, S. & Hallett, P. E. (1985). A schematic eye for the mouse, and comparisons with the rat. *Vision Research, 25*, 21–31.

Richards, D. W., Russell, S. R. & Anderson, D. R. (1988). A method for improved biometry of the anterior chamber with a Scheimpflug technique. *Investigative Ophthalmology and Visual Science, 29*, 1826–1835.

Rolls, E. T. & Cowey, A. (1970). Topography of the retina and striate cortex and its relationship to visual acuity in rhesus monkeys and squirrel monkeys. *Experimental Brain Research, 10*, 298–310.

Schaeffel, F., Glasser, A. & Howland, H. C. (1988). Accommodation, refractive error and eye growth in chickens. *Vision Research, 28*, 639–637.

Scheimpflug, T. (1906). Der Photoperspektograph und seine Anwendung. *Photographische Korrespondenz, 43*, 516.

Schein, S. J. (1988). Anatomy of macaque fovea and spatial densities of neurons in foveal representation. *Journal of Comparative Neurology, 269*, 479–505.

Sivak, J. G., Howland, H. C., West, J. & Weerheim, J. (1989). The eye of the hooded seal, *Cystophora cristata*, in air and water. *Journal of Comparative Physiology A, 165*, 771–777.

Southall, J. P. C. (1943). *Mirrors, prisms and lenses: A text-book of geometrical optics*. New York: Macmillan.

Troilo, D., Howland, C. & Judge, S. (1993). Visual optics and retinal cone topography in the common marmoset (*Callithrix jacchus*). *Vision Research, 33*, 1301–1310.

Vakkur, G. J. (1967). Studies on optics and neurophysiology of vision. M. D. Thesis, University of Sydney.

Acknowledgements—P.L. was entirely supported and S.J.S. was partially supported by NIH grant R01 EY06096 to S.J.S. We thank Dennis Thayer at the Jules Stein Eye Institute for performing Scheimpflug photography. We also thank Nancy London at the Jules Stein Eye Institute for performing ultrasound and keratometry. We are grateful to Pooneh Esfahani for her assistance in the preparation of some of the illustrations. Finally, we thank Dr Abbie Angharad Hughes for generously providing editorial help.